Fuzzy Ring-Overlapping Range-Free (FRORF) Localization Method for Wireless Sensor Networks

Andrija S. Velimirovic, Goran Lj. Djordjevic, Maja M. Velimirovic, Milica D. Jovanovic

University of Nis, Faculty of Electronic Engineering, Aleksandra Medvedeva 14, P.O. Box 73, 18000 Nis, Serbia

Abstract

The sensor node localization with an acceptable accuracy is a fundamental and important problem for location-aware applications of Wireless Sensor Networks (WSNs). Among numerous localization schemes proposed specifically for WSNs, the Received Signal Strength (RSS) based range-free localization techniques have attracted considerable research interest for their simplicity and low cost. However, these techniques suffer from significant estimation errors due to low accuracy of RSS measurements influenced by irregular radio propagation. In order to cope with the problem of RSS uncertainty, in this paper we propose a fuzzy set-based localization method, called Fuzzy Ring Overlapping Range Free (FROFR) localization. Similar to other area-based localization schemes, FRORF relies on beacon signals broadcasted by anchors to isolate a region of the localization space where the sensor node most probably resides. As an extension to the concept of ring-overlapping localization, FRORF first represents overlapping rings as fuzzy sets with ambiguous boundaries in contrast to fixed intervals of RSS values, and then generates fuzzy set of regions by intersecting rings from different fuzzy ring sets. The degrees of sensor node membership to regions in the fuzzy set of regions are used to determine the location estimate. The results obtained from simulations demonstrate that our solution improve localization accuracy in the presence of radio irregularity, and even for the case without radio irregularity.

Key words: wireless sensor networks, localization, RSS, ring-overlapping localization, fuzzy set theory.

1 INTRODUCTION

Recent advances in wireless communications, low-power design, and micro-electro-mechanical systems (MEMS) have enabled the development of relatively inexpensive and low power wireless sensor nodes. The common vision is to create a large Wireless Sensor Network (WSN) through *ad-hoc* deployment of hundreds or thousands of such tiny devices able to sense the environment, compute simple tasks and communicate with each other in order to achieve some common objective, like environmental monitoring, target tracking, detecting hazardous chemicals and forest fires, and monitoring seismic activity, military surveillance [1]. Most of these applications require the knowledge on the position of every node in the WSN [2]. Determining the physical positions of sensor nodes is one of the key issues in WSN operation because the position information is used: (i) to correlate sensor readings with physical locations, (ii) in location-aided routing and data aggregation, and (iii) to make easier network self-configuration and self-organization. Also, in many applications such as inventory management and target tracking, the position itself is the information of interest.

However, in most cases, sensor nodes are deployed throughout some region of interest without their position information known in advance. Thus, the first task that has to be solved after network deployment is to localize the nodes, i.e., to find out their spatial coordinates in some fixed coordinate system. The locations of nodes can be set manually but this is not practical for large scale WSNs. Another possible way to localize sensor nodes is to use the commonly available Global Positioning System (GPS), which offers 3-D localization based on direct line-of-sight with at least four satellites [3]. However, attaching a GPS receiver to each sensor node is highly impractical solution due to its high power consumption, high price, inaccessibility (nodes may be deployed indoors, or GPS reception might be obstructed by climatic conditions), and imprecision (the positioning error might be of 10-20m) [4].

A number of self-localization systems and algorithms have been proposed recently specifically for WSNs, which are generally classified into range-based and range-free localization schemes [5]. The range-based localization depends on the assumption that sensor nodes have the ability to estimate the distance or angle to other nodes by means of one or more of the following measurements: angle of arrival (AoA), time of arrival (ToA), time difference of arrival (TDoA), and received signal strength (RSS) [6]. Approaches based on the first three types of measurements are not widespread in WSNs because they require installation of specific and

expensive hardware such as array antennas for AoA [7], ultrasound for TDoA [8], and dedicated hardware and software to maintain node synchronization [9]. On the other hand, RSS-based localization systems are much more popular since most of today's radio transceiver chips for WSNs provide received signal strength indicator (RSSI) circuitry at no extra hardware cost. However, the distance estimated by RSSI is usually inaccurate and unreliable [10,11,12]. This is because the RSS is subject to negative effects of radio interference, obstacles (e.g. persons, walls), and individual differences of transmitters and receivers (e.g. antenna type, transmission power).

Similar to RSSI range-based technique, the majority of range-free approaches are based on reusing radio communication to enable location-unknown sensor nodes to determine their locations with the assistance of a sufficient number of anchors (i.e. location-aware nodes) [13]. In contrast to range-based techniques, the range-free localization schemes do not rely on absolute estimates of distances. Instead, these schemes enables sensor nodes to infer their locations by exploiting radio connectivity information among nodes, anchor proximity, near-far information, comparison of either RSSI readings or less accurate distance estimation. Range-free solutions use only standard features found in most radio modules as hardware means for localization, thus providing more economic and simpler location estimates than the range-based ones. On the other hand, the results of range-free methods are not as precise as those of the range-based methods.

Among numerous range-free methods, anchor proximity [14,15,16] and radio connectivity-based solutions [4,17,18] feature a low overall system cost, however, by sacrificing localization accuracy. In centroid localization method, all anchors first send out beacon messages that include their position information to all sensor nodes within their transmission range [14]. Then, all sensor nodes calculate their own position as the geometric centroid of a polygon whose vertices are the anchors in range. To achieve a good accuracy, however, a high anchor density is required, which is impractical for large-scale systems. In [15], each anchor emits beacon signals at different transmission power levels. After receiving the beacon signals, a node can determine in which annular ring it is located within each anchor node and uses the geometric center of the intersection of the rings as its position estimate. In [16], a multi-power level mobile anchor assisted range-free algorithm is proposed. The algorithm is based on convex optimization and uses a relay node to reduce the effect of obstacles on node localization. Connectivity-based methods use local neighborhood sensing to build hop-based virtual

distances for large-scale sensor network localization. In DV-Hop algorithm, anchors first flood their location throughout the network, and then each sensor node calculates its position based on received anchor locations, the hop count on the shortest multi-hop path from the corresponding anchor, and the average distance per hop [4]. The method proposed in [18] improves connectivity-based methods by extracting the relative distance information from neighborhood orderings obtained from RSS sensing. The advantage of these schemes lies in their simplicity. However, they can provide acceptable location estimation accuracy if the radio transmission range is constant and anchor/node distribution in the network is dense and uniform.

In area-based range-free localization approaches, unkonwn nodes perform location estimation by partitioning the environment into a number of overlapping localization areas. A node's presence inside or outside of these areas allows a node to narrow down the region in which it can potentially reside. The correctness of the area-based schemes is based on the assumption that as the distance between a transmitter and a receiver increases, the signal strength measured by the receiver decreases monotonically. This assumption is called monotonicity constraint and is used to obtain the relative spatial relationship between anchors/nodes. For example, in APIT algorithm, each node decides its position based on the possibility of being inside or outside of a triangle formed by any three anchors heard by the node [5]. To determine whether a node position falls within the triangle, APIT compares the RSSI readings from the anchors at the node with those at its neighbors. In ROCRSSI algorithm, a localization region is defined as the intersection area of overlapping annular rings which constrain the position of the sensor node with respect to each anchor [19]. The rings are generated by comparison of the signal strength a sensor node receives from a specific anchor and the signal strength other anchors receive from the same anchor. Area-based localization techniques can provide a better location accuracy even there is an random anchor placement. However, in order to compensate for negative effects of irregular radio propagation and inaccurate RSSI measurements, they require a high anchor-to-node ratio which results in high cost.

An approach to tackle the problem of RSS inaccuracy due to varying environmental conditions is proposed in [20]. In this range-based method, RSSI is used to calculate the distances between nodes at unknown positions and anchors according to a simple signal propagation model. The set of anchors and reference nodes placed at known positions are used to estimate attenuation parameters of the signal propagation model in a closed-loop feedback correction manner. To tolerate environmental variations, the parameter estimations are updated periodically and

distributed to unknown nodes. A range-free localization approach that explicitly deals with RSSI inaccuracy by employing soft computing techniques is described in [21]. They have proposed an enhanced centroid localization method using edge weights of adjacent anchor nodes based on Takagi-Sugeno-Kang (TSK) fuzzy modeling. The method uses fuzzy membership function which is optimized by means of genetic algorithm to transform RSSI information into edge weights. Then, a weighted centroid method is employed to localize the node. In the second scheme introduced by the same authors, the entire sensor location mapping from the anchor node signals is approximated by a neural network [22].

In this paper we propose a distributed range-free, area-based localization technique, called Fuzzy Ring Overlapping Range Free (FRORF) Localization, which utilizes the RSSI to estimate the position of a sensor node with respect to a small number of randomly distributed anchors. Similar to other area-based localization methods [5,15,19], FRORF uses beacon signals broadcasted by anchors to isolate a region of the localization space where the sensor node most probably resides. Like in ROCRSSI algorithm, localization regions correspond to intersection areas of overlapping rings. To test whether the sensor node location is inside or outside of the specific ring is based on the comparison of the signal strength a sensor node receives from the anchor placed in ring's center with the signal strength other anchors receive from the same anchor. The novelty of our localization scheme is to represent overlapping rings as fuzzy sets with ambiguous boundaries in contrast to fixed intervals of RSSI values (which are used in ROCRSSI). The use of the fuzzy set theory is motivated by the need to enhance performance of the area-based localization approach through explicit modeling of uncertainty in RSSI measurements, caused by irregular radio propagation, in an efficient and natural way. The irregularity of the radio propagation creates rings with non-circular borders and might induce a significant localization error when a binary decision-making model (i.e., "in-ring" versus "out-of-ring") is employed, like in ROCRSSI. In our approach, we first use fuzzy membership functions, based on the RSSI information, to calculate the degrees to which the sensor node location falls within different rings. Then we apply a sequence of basic fuzzy set operations to derive the degrees of sensor node membership to different localization regions. Finally, we use these degrees as weights of localization regions, and set the estimated position of the sensor node in the center of gravity of the localization space.

The rest of the paper is organized as follows: Section 2 introduces localization based on comparison of RSS measurements and discuses how fuzzy set theory can be applied to this range-free approach. Section 3 presents the FRORF localization algorithm. Simulation results

for various scenarios used to evaluate performance of FRORF algorithm are presented in Section 4. We conclude our paper in Section 5.

2 LOCALIZATION BASED ON COMPARISON OF RSS

RSS–based range–free algorithms only rely on the assumption that the RSS is a decreasing function of the distance between transmitter and receiver. For example, if the straight of the beacon signal that sensor node *S* receives from anchor A_1 is greater than the straight of the same signal received by anchor A_2, then *S* can conclude that it is closer to A_1 then A_2. A number of distance constraints, produced after a series of such comparisons, will enable the sensor node to confine its position within a limited area of the localization space.

Let's consider a network with $N = 3$ anchors placed at fixed known positions in 2-D localization space shown in Fig. 1. Around each anchor the set of $N - 1$ concentric circles is placed. Radius of every circle equals distance between the center anchor and one of $N - 1$ remaining (peripheral) anchors. Each set of concentric circles partitions the localization space into N rings numbered from 1 to N. The ring 1 corresponds to the area of the innermost circle, while the ring N corresponds to the outside area of the last circle. A localization region is the intersection area of rings from different ring sets, while its area code is the sequence of the intersecting ring numbers, i.e. ring ranks. For example, shaded area in Fig. 1 represents the region with the area-code (2, 1, 2), i.e. the region which is obtained by intersecting rings 2, 1 and 2 of anchors A_1, A_2, and A_3, respectively. Note that for each point p in this region, the area-code (2, 1, 2) defines the following set of distance-based constraints:

$$d(A_1, A_2) \leq d(A_1, p) \leq d(A_1, A_3)$$

$$d(A_2, A_2) \leq d(A_2, p) \leq d(A_2, A_3)$$

$$d(A_3, A_2) \leq d(A_3, p) \leq d(A_3, A_1)$$

where $d(x, y)$ denotes the distance between two anchors/nodes. Note also that localization regions differ in size and shape, and their total number depends on the constellation of anchors.

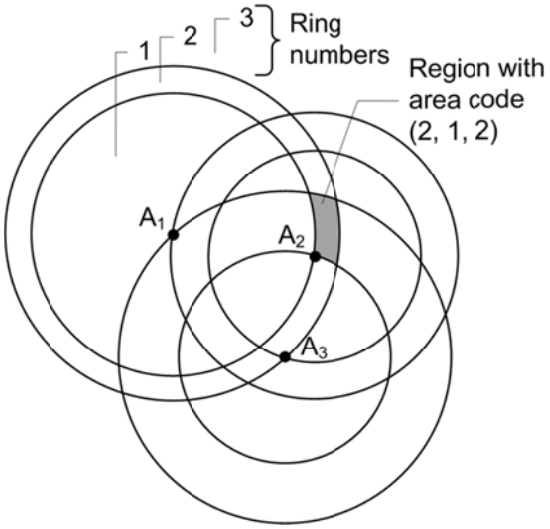

Fig. 1. Rings, regions and area-codes.

In an idealistic physical environment, RSS measured at a point further from an anchor is always smaller then RSS measured at a point that is closer to the same anchor. As a consequence, if we use RSS information for the regionalization of the localization space, the resulting set of regions, i.e. the set of region area codes, will be the same as one obtained by using distance information. This means that a sensor node will always be able to locate itself into the correct localization region by using the comparison of RSS values, only. For example, the following set of RSS-based constraints will confine the location of the sensor node *S* inside the region (2, 1, 2) of the network given in Fig. 1:

$$rss(A_1, A_3) \leq rss(A_1, S) \leq rss(A_1, A_2)$$

$$rss(A_2, A_3) \leq rss(A_2, S) \leq rss(A_2, A_2)$$

$$rss(A_3, A_1) \leq rss(A_3, S) \leq rss(A_3, A_2)$$

where $rss(x, y)$ denotes the strength of the signal broadcasted by anchor x as measured by anchor/node y. Note that the correctness of the ring selection is preserved as long as the monotonicity constraint between the Euclidean distance and the RSS is satisfied, which means that whenever $d(x, y) < d(x, z)$ then it should never be the case that $rss(x, y) < rss(x, z)$.

However, the radio propagation is usually not homogenous in all directions because of the presence of multi-path fading and different path losses depending on the direction of propagation. An irregular radio propagation pattern may have significant impact on the accuracy of a area-based localization since the monotonicity constraint is no longer guaranteed. The

consequence might be a selection of a wrong ring and eventually localization of a sensor node in a wrong region. Let's consider a partial distance-based regional map of the network configuration with four anchors given in Fig. 2. A sensor node *S*, depicted with a square mark, is located in the region with area-code (3, 1, 1, 3). However, due to inaccurate RSS measurements, *S* may easily came up with the wrong decision regarding its regional area-code. For example, in order to correctly locate itself into ring 3 of the anchor A_4, *S* should measure the lower strength of the beacon signal broadcasted by A_4 then anchor A_3. However, because of the irregularity in radio propagation, there is a chance for *S* to measure a higher RSS then A_3. Such an imprecision will cause the sensor node *S* to choose the area-code (3, 1, 1, 2) instead of the correct one (3, 1, 1, 3). As *S* is closer to the boundary of the A_4's ring 3 the chance for the wrong ring selection is greater. Note that the area-code (3, 1, 1, 2) is ***valid***, but ***wrong*** in this case. Under some circumstances, *S* may pick an area-code that does not even exist in distance-based regional map, i.e. it may select so called ***invalid*** area-code. For example, an incorrect ring selection with respect to anchor A_2 could result in the area-code (3, 2, 1, 3). It is easy to see that this area-code does not exist in the given regional map since 3rd rings of anchors A_1 and A_4 intersect in two regions, only, i.e. in regions (3, 1, 1, 3) and (3, 4, 4, 3).

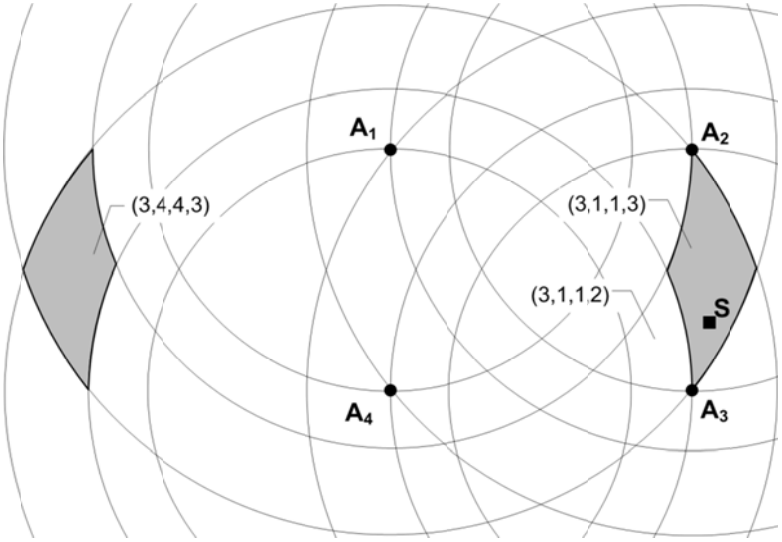

Fig. 2. A segment of distance-based regional map.

The problem could be even worse if two or more anchors are at similar distances from the central one. In that case it might happen that the measured RSS value by the closer anchor is less than the measured RSS value by the further anchor. As a result, the ordering of the anchors based on comparison of RSS values might not be identical with their ordering based on

comparison of Euclidean distances, which might increase localization errors. Let consider again the network configuration shown in Fig. 2, and suppose that the monotonicity constraint between anchors A_2 and A_3 with respect to A_1 is violated. This means that $rss(A_1, A_2) < rss(A_1, A_3)$ in spite of $d(A_1, A_2) < d(A_1, A_3)$. As a result of this radio propagation anomaly, the sensor node *S* will not be able to select its *home* ring A_2-A_3 centered in A_1 since the corresponding RSS-based constraint $rss(A_1, A_2) > rss(A_1, S) > rss(A_1, A_3)$ is not satisfied for any $rss(A_1, S)$. Instead, *S* choice will be either ring A_1-A_2, when $rss(A_1, A_2) < rss(A_1, S)$, or ring A_3-∞, when $rss(A_1, S) < rss(A_1, A_3)$, or even both rings A_1-A_2 and A_3 - ∞, when $rss(A_1, A_2) < rss(A_1, S) < rss(A_1, A_3)$. This will definitely cause that the sensor node *S* will be placed into a wrong region or wrong regions.

In ROCRSSI algorithm, the problem of incorrect ring/region selection is solved by choosing the valid region (or regions) with the maximum number of intersecting rings. However, in this approach, a small radio irregularity in the proximity of ring boundaries may lead to a large localization error, as illustrated in Fig. 3(a).

In order to overcome the uncertainty of the RSS and the nonlinear relationship between the RSS and the distance, in this work we suggest a different approach based of the fuzzy theory. We use fuzzy sets to model the relationship between localization regions and the RSS information available to the sensor node. When comparing its RSS measurements with those of anchors, the sensor node will not select one region only, but it might choose one or more regions each with equal or different *weights* representing certainty of the decision. This concept is illustrated in Fig. 3(b). Different shades of gray indicate different weights of the selected regions. Finally, the Center of Gravity (CoG) of the shaded area is used as the final location estimation.

(a) (b)

Fig. 3. ROCRSSI vs. fuzzy based selection (FRORF) of localization regions.

3 FRORF ALGORITHM FOR SENSOR NODE LOCALIZATION

In this section, we present our fuzzy set-based range-free localization scheme, which we call Fuzzy Ring Overlapping Range Free (FRORF) localization. FRORF requires a heterogeneous WSN composed of two sets of static nodes distributed across a planar localization space: a set of *N* anchors, i.e. the nodes whose locations are known and accurate, and a set of sensor nodes, i.e. the nodes whose locations are to be determined. Sensor nodes estimate their positions only based on the information received from the anchor nodes. Since our method does not depend on neighboring sensor node communication, it is independent of network connectivity. For simplicity and ease of presentation we limit the localization space to 2-D, but with minor modifications our algorithm is capable of operating in 3-D. Anchor nodes, or nodes with *a prior* knowledge of their locations in the localization space (obtained via GPS or other means such as pre-configuration), serve as reference points, broadcasting beacon messages. Anchors are assumed to be sparse and randomly located. Both anchors and sensor nodes are equipped with omni-directional antennas and RF transceivers with built-in RSSI circuitry. In addition, as in the case of some other schemes (e.g. [15,19]), anchors are assumed to have a larger communication range than normal sensor nodes so that their beacons can reach all wireless nodes in the network. The need for larger communication range and the optional use of GPS receiver to localize anchors make such nodes more expensive, consuming more energy, and being larger in size than normal sensor nodes.

High level overview of FRORF is illustrated in Fig. 4. FRORF operation can be divided into two phases: (a) beacon exchange phase, and (b) computation phase. The first phase involves measuring RSS from anchors and distributing both RSS data and anchors' location information to all sensor nodes in the network. After completion of the beacon exchange phase, each sensor node has enough information needed to perform the computation phase all by itself. At the first computation step, the sensor node uses location information of anchors to partition the localization space into the set of localization regions, i.e. to generate so-called distance-based regional map. Then, FRORF employs a fuzzy-set based procedure to estimate location of the sensor node. This procedure takes three steps: (a) fuzzification; (b) fuzzy inference, and (c) defuzzification. In the fuzzification step, every ring is represented as a fuzzy set, referred to as *fuzzy ring*, associated with suitably selected membership function. Then, degrees of sensor node membership to every fuzzy ring are calculated using available RSSI data and known anchors locations. The outputs of this step are *N fuzzy-ring sets*, each one of which includes fuzzy rings around one anchor with nonzero degree of sensor node membership. In the fuzzy

inference step, fuzzy set of regions is generated by intersecting fuzzy rings from different fuzzy-ring sets, and degree of sensor node membership to each fuzzy region is derived. In the final step, the location of the sensor node is calculated by using the center of gravity defazzification technique.

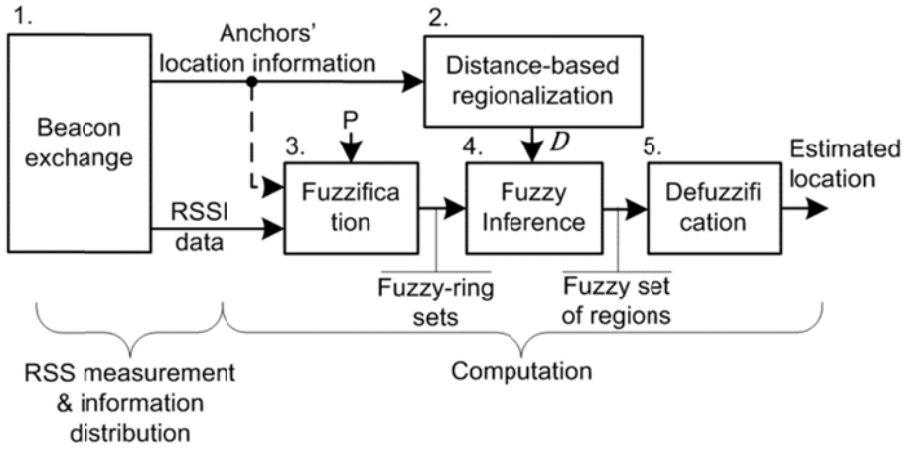

Fig. 4. High level overview of FRORF.

3.1 Beacon Exchange

The FRORF algorithm requires every anchor to periodically send out a beacon message including its own ID. While receiving the beacon message, every other anchor and every sensor node samples the RSS and stores the measured value together with the ID of the transmitting anchor. After all anchors transmitted their beacon messages, each anchor broadcasts so-called localization message to all sensor nodes. The localization message includes anchor's ID and its own location information, along with a vector containing the recorded RSS values of beacons it received from other anchors. We assume that anchors are synchronized (e.g. via GPS if installed or using some other synchronization method [23]) so that their beacon and localization message transmissions do not overlap in time. After completion of beacon exchange phase, each sensor node *S* has enough information needed to perform localization by itself. This information includes not only locations of all anchors, but also RSS values measured between each pair of anchors, as well as RSS values from all anchors as measured by sensor *S*, i.e.:

- Vector $[l_i]_N$ of anchor locations wherein $l_i = (xa_i, xa_i), i = 1, \dots, N$, is 2-D coordinates of anchor A_i in the localization space.
- Vector $[\rho_i]_N$ of sensor node's RSSI readings wherein $\rho_i, i = 1, \dots, N$, is the strength of the beacon signal that S received from anchor A_i.

- Matrix $[r_{i,j}]_{N\times N}$ of anchors' RSSI readings wherein $r_{i,j}, i,j = 1,\dots,N$, is the strength of the signal that anchor A_j received form anchor A_i.

3.2 Distance-Based Regionalization

After collecting enough information, the sensor node can start the localization process. The first step in this process is to create a distance-based regional map of the localization space by using the known locations of all anchors. Let $AS = \{A_i | i = 1, \dots N\}$ be the set of anchors. Taking A_i as the *center anchor*, elements in *AS* can be arranged into the anchor sequence $Q_i = (a_0 = A_i, a_1, \dots, a_{N-1}, a_N = F)$ in order of their distances from A_i, wherein $a_j \in AS\backslash\{A_i\}, j = 1, \dots, N-1$, and *F* is a fictive anchor placed in infinity. Thus, $d(A_i, a_j) \leq d(A_i, a_{j+1})$ holds for any two anchors $a_j, a_{j+1} \in Q_i$. Each anchor sequence $Q_i, i = 1, \dots, N,$ defines an ordered sequences of distance-intervals $T_i = ([0, d(A_i, a_1)], \dots, \left[d\left(A_i, a_j\right), d\left(A_i, a_{j+1}\right)\right], \dots, [d(A_i, a_{N-1}), \infty])$. For any point *p* in the localization space and any anchor A_i, there exists exactly one distance-interval in T_i such that $d(A_i, a_j) \leq d(A_i, p) \leq d(A_i, a_{j+1})$. The ordinal number of that distance-interval in T_i represents the rank of point *p* with respect to anchor A_i, written as $rank_i(p)$. The *area-code* of point *p*, written as $c(p)$, is defined as the sequence of its ranks with respect to all anchors in *AS*, i.e. $c(p) = (rank_0(p), \dots, rank_{N-1}(p))$. Note that the order in which the ranks are listed in an area-code is determined by a predefined order of anchor IDs. *Localization region*, *R*, with area code C is the set of all points in the localization space with the same area-code, i.e. $R = \{p | c(p) = C\}$. Distance-based regional map, denoted as $\mathcal{D}$, is the set of area-codes of all regions identified in the localization space.

For the purpose of the proposed localization algorithm, each localization region needs to be associated with the following two attributes: (a) the area-code, and (b) the Center of Gravity (CoG). The CoG of a region *R* is the average location of all points in *R*. Since the analytical procedure for finding regions and calculating their CoGs is rather computationally involved for resource constrained sensor nodes, due to the large number of floating point operations, we adopted an approximate approach based on grid-scan method [5,19]. In this method, the localization space is divided into the uniform grid array, and the center of a grid, which is called grid point, represents the area of that grid. Initially, the distance-based regional map, $\mathcal{D}$, is empty. In order to identify localization regions, the grid array is scanned, point-by-point. For each grid point *p* with coordinates $(x(p), y(p))$ the area-code $c(p)$ is first determined based on its Euclidean distances to the anchors, and then the regional map $\mathcal{D}$ is searched for a region with

that area-code. If the area-code $c(p)$ is not found in $\mathcal{D}$, then the new localization region with the area-code $c(p)$ is created and inserted into the map. During construction of $\mathcal{D}$, the following four variables are associated with each region: *C* - area-code; *X* and *Y* - sums of x- and y-coordinates of all grid points in the region, respectively, and *G* - the number of grid points in the region. When the new region is created, these variables are initialized as: $C = c(p), G = 1, X = x(p), \text{and } Y = y(p)$. Otherwise, if $\mathcal{D}$ already contains the region with the area-code $c(p)$, then variables *X*, *Y*, and *G* of that region are updated as follows: $G = G + 1, X = X + x(p), \text{and } Y = Y + y(p)$. After grid scanning is completed, the coordinates of the region's CoG are calculated as $\left(\frac{X}{G}, \frac{Y}{G}\right)$.

Note that the computation load of sensor nodes can be reduced at the expense of communication cost, if $\mathcal{D}$ is generated by an anchor at the end of the beacon exchange phase, and then distributed to all sensor nodes.

3.3 Fuzzification

In this section we present the fuzzy set based method used in FRORF to estimate the location of the sensor node based on RSS data and known anchor-to-anchor distances.

3.3.1 Fuzzy Ring

As demonstrated in Section 2, the crisp conditions that restrict the location of a sensor node within the area of a ring can be expressed as $x \in RI$, where $RI = [\alpha, \beta]$ is so called ring interval; α and β are positive real-valued numbers defining ring boundaries, and x is so called *sensor crisp value* (see Fig. 5). Boundary values $\alpha, \beta \in R^+$ are associated with ring's two peripheral anchors representing a measure of their distances from the center anchor (e.g. Euclidean distances or RSS values). The sensor crisp value x expresses an estimation of the sensor node's distance from the ring's center given in the same units as α and β. Also, we can associate two wider intervals $LT = [0, \beta]$, and $GT = [\alpha, \infty]$ with the ring. Intervals LT and GT correspond to the inner area of the outer ring's circle and the outer area of the ring's inner circle, respectively. Obviously, $RI = LT \cap GT$.

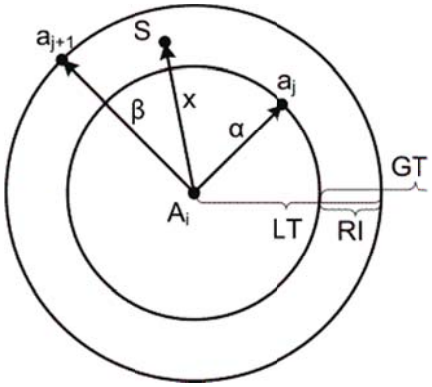

Fig. 5. Ring parameters.

We start building our fuzzy model by representing crisp intervals LT and GT as fuzzy sets $\widetilde{LT} = \{(x, \mu_{LT}(x))|x \in R^+\}$ and $\widetilde{GT} = \{(x, \mu_{GT}(x))|x \in R^+\}$, where $\mu_{LT}(x)$ and $\mu_{GT}(x)$ are membership functions defined as follows:

$$\mu_{LT}(x) = \begin{cases} 1 & if \quad x \leq \beta(1-P) \\ \dfrac{(1+P)\beta - x}{2P\beta} & if \quad \beta(1-P) < x < \beta(1+P) \\ 0 & if \quad x \geq \beta(1+P) \end{cases}$$

$$\mu_{GT}(x) = \begin{cases} 0 & if \quad x \leq \alpha(1-P) \\ \dfrac{x - (1-P)\alpha}{2P\alpha} & if \quad \alpha(1-P) < x < \alpha(1+P) \\ 1 & if \quad x \leq \alpha(1+P) \end{cases}$$

A fuzzy ring is defined as the fuzzy set derived by applying the fuzzy intersection operation on fuzzy sets $\widetilde{LT}$ and $\widetilde{GT}$:

$$\widetilde{RI} = \widetilde{LT} \cap \widetilde{GT} = \{(x, \mu_{RI}(x))|x \in R^+\}$$

For the membership function $\mu_{RI}(x)$ we use:

$$\mu_{RI}(x) = \mu_{LT}(x) + \mu_{GT}(x) - 1 \qquad (1)$$

Note that expression (1) is known in fuzzy set theory as bounded product (or bold intersection) [24].

A graphical interpretation of membership functions $\mu_{RI}(x)$, $\mu_{LT}(x)$, and $\mu_{GT}(x)$ is given in Fig. 6. Parameter P, which we call the level of fuzzification, is involved to enable adaptation to various degrees of radio propagation irregularity. The value of $P \in [0,1]$ controls the width of the fuzzy

region in vicinity of ring boundaries, α and β. A sensor node uses functions $\mu_{LT}(x)$ and $\mu_{GT}(x)$ when it compares its crisp value x with the ring boundary values α and β. When the sensor crisp value is outside the fuzzy region, the outcome of this comparison is strictly "less then" or "greater then" indicating the full membership or full non-membership in $\widetilde{LT}$ and $\widetilde{GT}$. On the other hand, when the sensor crisp value is within the fuzzy region, the result of the comparison is a partial membership in $\widetilde{LT}$ or $\widetilde{GT}$. When fuzzy regions of $\mu_{LT}(x)$ and $\mu_{GT}(x)$ do not overlap, the result of their intersection is a trapezoidal type membership function $\mu_{RI}(x)$, as shown in Fig. 6(a). In this case, there is a range of x within the interval $[\alpha, \beta]$ with the full membership in the corresponding fuzzy ring. Otherwise, if fuzzy regions of $\mu_{LT}(x)$ and $\mu_{GT}(x)$ overlap, then the membership function $\mu_{RI}(x)$ takes the shape of an irregular quadrilateral (see Fig. 6(b)). In this case, the height of $\mu_{RI}(x)$ is less than 1 indicating that there is no value of x such that the sensor node may assume the full membership in the corresponding fuzzy ring. As the ring boundary values get closer to each other, the height of $\mu_{RI}(x)$ becomes smaller and smaller approaching the zero.

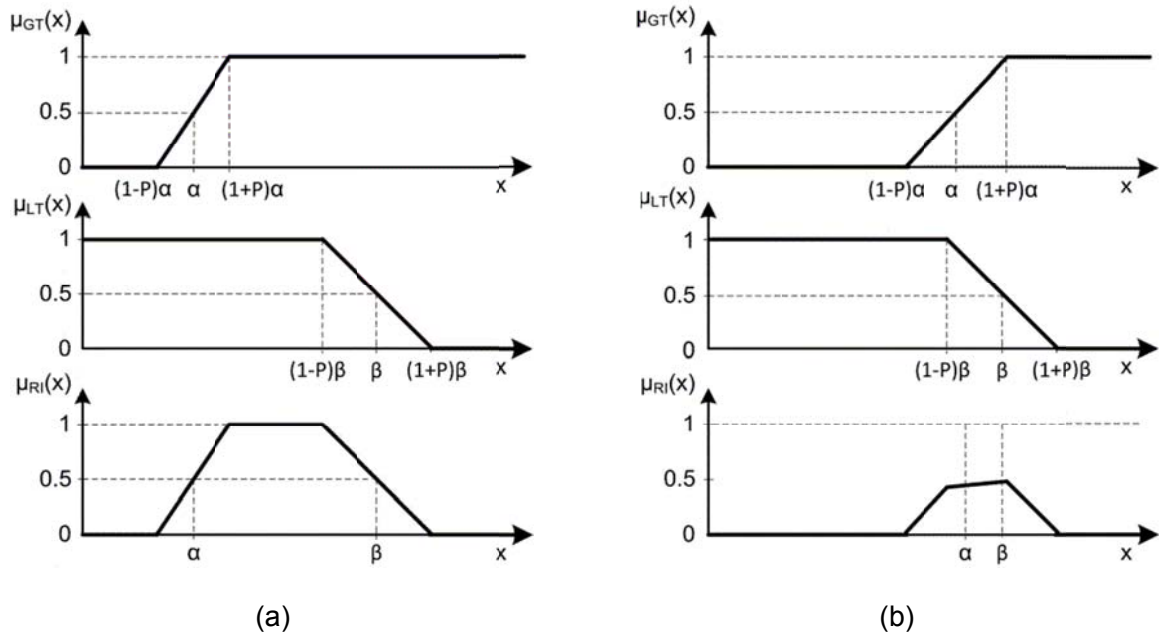

Fig. 6. Membership functions for fuzzy ring: (a) non-overlapping fuzzy regions of $\boldsymbol{\mu_{LT}(x)}$ and $\boldsymbol{\mu_{GT}(x)}$; (b) overlapping fuzzy regions of $\boldsymbol{\mu_{LT}(x)}$ and $\boldsymbol{\mu_{GT}(x)}$.

Fig. 7 shows a composition of fuzzy-ring membership functions along a particular anchor sequence. Using the crisp comparisons, three different sensor crisp values, x_1, x_2, and x_3, will be mapped into three different rings, 0, 1 and 2, respectively. Although we may have a high degree of confidence in such mapping as sensor crisp value x_2 is concerned, the mappings of x_1 and x_3

are much more uncertain due to their proximity to the ring boundaries. On the other hand, the mapping based on fuzzy membership functions explicitly models the uncertainty in sensor crisp values and might map the sensor location into two or even more than two fuzzy rings if the input value is close enough to one or more ring boundary values. As illustrated in Fig. 7, due to proximity to the ring boundary value a_1, sensor crisp value x_1 is not only mapped into the fuzzy ring 0, but also mapped into the fuzzy ring 1, although with a smaller degree of membership in fuzzy ring 1. The fuzzification of the sensor crisp value x_3, which falls into the narrow crisp ring interval $[a_2, a_3]$ with overlapping boundary fuzzy regions, maps the sensor node location into three fuzzy rings, 1, 2 and 3, all with different degree of membership.

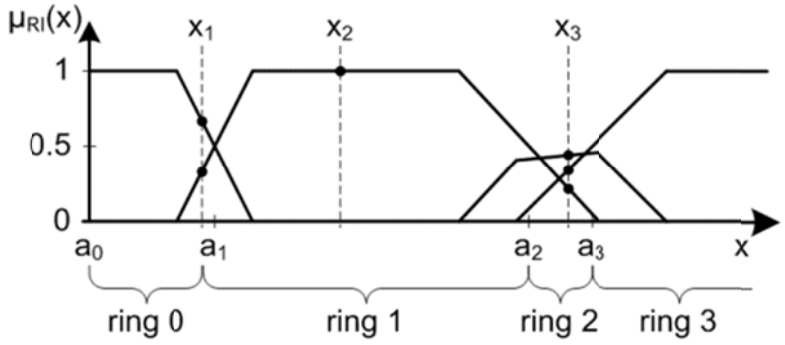

Fig. 7. Derivation of fuzzy-ring set for three different sensor crisp values.

The proposed method of fuzzification is quite general since it does not specify which data to use for the ring boundary values, α and β, and the sensor crisp value x. In the sequel, we propose two approaches on how to utilize the information available to a sensor node in order to derive the values of α, β and x.

1) Direct-RSS Fuzzification: In this approach, the fuzzification is performed by using row RSS measurements, only. Let ρ_i and $r_{i,j}$ be RSSI values of A_i's beacon signal as measured by the sensor node, and jth anchor in the anchor sequence headed in A_i, respectively. We assume that $r_{i,0} = \infty$, and $r_{i,N} = 0$. The degree of sensor node membership to the jth fuzzy ring of the anchor A_i, written as $\mu_{RI}^{i,j}$, is calculated as follows:

$$\mu_{RI}^{i,j} = \mu_{RI}(x), \text{ where } x = \rho_i, \alpha = Min\{r_{i,j}, r_{i,j+1}\}, \text{ and } \beta = Max\{r_{i,j}, r_{i,j+1}\}$$

2) Indirect-RSS Fuzzification: This fuzzification approach tends to enhance the precision of the RSS to fuzzy ring mapping by involving known and accurate anchor-to-anchor distances into the fuzzification process. This is accomplished by defining fuzzy rings in the Euclidean domain, and

converting sensor node's RSS measurements into distances. Let $d_{i,j}, j = 0, \ldots N$, be the Euclidean distance between anchor A_i and jth anchor in the anchor sequence headed in A_i. Then, the boundary values of the jth fuzzy ring of A_i are $\alpha = d_{i,j}$ and $\beta = d_{i,j+1}$. We assume $d_{i,0} = 0$, and $d_{i,N} = \infty$. Also, when determining degree of a sensor node membership to jth fuzzy ring of anchor A_i, the sensor crisp value x should represent the estimation of its distance to A_i. This distance estimation is obtained (similar to the approach presented in [20]) by correlating sensor node's RSS measurement of the A_i's beacon signal with those of A_i's peripheral anchors, as will be explained below.

In order to convert sensor node's RSS measurements into distances from anchors we rely on the basic circular radio propagation model which assumes that RSS attenuates with transmitter-receiver distance d as d^{γ} where γ is the path loss exponent that depends on the environment through which the RF signal is propagated. For free space it is well known that $\gamma = 2$. For a non-free space area, the path loss exponent is varying between 2 and 5 depending on the environment, which is usually determined by experimental field measurements. Following this model, locations with the same RSS value form perfect circles centered at the transmitter. Therefore, RSS values and distances from the transmitter at any two points $p1$ and $p2$ in the RF field are related via the expression:

$$\frac{rss_1}{rss_2} = \left(\frac{d_2}{d_1}\right)^{\gamma} \tag{2}$$

Accordingly, the distance between the sensor node and anchor A_i can be inferred from RSS by taking one of peripheral anchors, say a_j, as the reference receiver:

$$\delta_i = d_{i,j} \sqrt[\gamma]{\frac{r_{i,j}}{\rho_i}} \tag{3}$$

However, in most environments, the radio propagation pattern is not circular, but quite irregular in shape. These variations of path loss in different directions of propagation are due to phenomena like reflections, diffraction, and scattering in the medium, as well as hardware calibration differences, non-isotropic antenna gain etc. As a consequence of the radio propagation irregularity, the proportion (2) may not be satisfied in all cases. In practice, if points $p1$ and $p2$ are aligned in similar directions with respect to the transmitter, the RSS-ratio and distance-ratio in (2) are approximately the same. Otherwise, these two ratios may differ significantly. Thus, if we chose a different anchor as the reference receiver in expression (3), we

might expect different distance estimation. Actually, we use this fact to calculate the set of $N-1$ distance estimations $\left\{\delta_i^{(k)} \mid k=1,\ldots,N-1\right\}$ for the sensor node from the anchor A_i having all other peripheral anchors as a referent anchor just once (see Fig. 8).

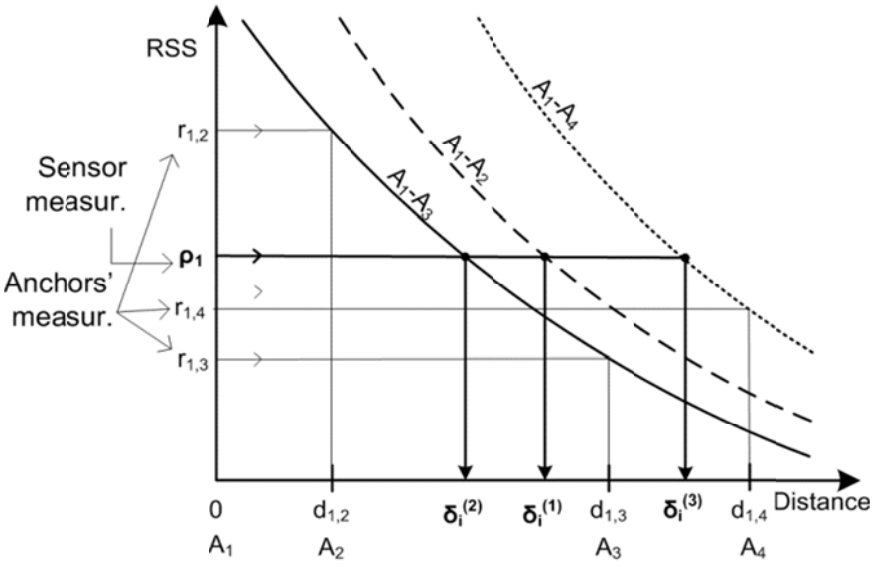

Fig. 8. Possible estimated distances of sensor S from anchor A_i due to various radio propagation characteristics in different direction of propagation.

Once the set of estimated distances is determined, these values are used as crisp input values in the process of defining the degree of sensor node membership to fuzzy-rings. However, due to redundancy in distance estimations, some form of averaging needs to be involved into the fuzzification process. We propose two such averaging methods:

- **F**irst Distance **A**veraging **t**hen **F**uzzification (FAtF), and
- **F**irst **F**uzzification **t**hen fuzzy ring membership **A**veraging (FFtA).

In FAtF method, the distance δ_i of the sensor node from the anchor A_i is first determined as the average of all distance estimations in $\left\{\delta_i^{(k)}\right\}$:

$$\delta_i = \frac{1}{N-1}\sum_{k=1}^{N-1}\delta_i^{(k)}$$

Then, the degree of sensor node membership to the jth fuzzy ring of the anchor A_i is calculated as:

$\mu_{RI}^{i,j} = \mu_{RI}(x)$, where $x = \delta_i, \alpha = d_{i,j}, \beta = d_{i,j+1}$

In FFtA method, the degree of sensor node membership to the jth fuzzy ring of the anchor A_i is first calculated for each distance estimation in $\left\{\delta_i^{(k)}\right\}$, separately, as follows:

$$(\mu_{RI}^{i,j})^{(k)} = \mu_{RI}(x), \text{ where } x = \delta_i^{(k)}, \alpha = d_{i,j}, \beta = d_{i,j+1}, \text{ and } k = 1, \dots, N-1$$

Then, the final degree of sensor node membership to the jth fuzzy ring of the anchor A_i is obtained by averaging over all calculated degrees:

$$\mu_{RI}^{i,j} = \frac{1}{N-1}\sum_{k=1}^{N-1}(\mu_{RI}^{i,j})^{(k)}$$

3.3.2 Fuzzy-Ring Set

The fuzzy-ring set of anchor A_i, $i = 1, \dots, N-1$, written as $\widetilde{RS}_i$, is the discrete fuzzy set containing ranks of all fuzzy rings of A_i with nonzero degree of sensor node membership, i.e.,

$$\widetilde{RS}_i = \left\{\left(j, \mu_{RI}^{i,j}\right) | \, \mu_{RI}^{i,j} > 0, j \in \{0, \dots, N\}\right\}$$

The level of fuzzification, P, is the main factor that influences the expected size of a fuzzy-ring set. The minimal size of a fuzzy-ring set is 1. This occurs when the sensor crisp value falls into the non-fuzzy area of one fuzzy ring, only (e.g. in, $x = x_2$ gives $\widetilde{RS}_i = \{(1,1.0)\}$). When the sensor crisp value is within the fuzzy region between two wide fuzzy rings, the typical size of the fuzzy-ring set is 2 (e.g. in Fig. 7, $x = x_1$ gives $\widetilde{RS}_i = \{(0,0.67), (1,0.33)\}$). When the sensor crisp value lies within the area of a narrow fuzzy ring, the resulting fuzzy-ring set usually includes three or more fuzzy rings (e.g., in Fig. 7, $x = x_3$ gives $\widetilde{RS}_i = \{(1,0.23), (2,0.44), (3,0.33)\}$). It is easy to verify that the sum of sensor node's membership degrees to all fuzzy rings in one fuzzy-ring set is always equal to 1.

3.4 Fuzzy Inference

The goal of this algorithm step is to calculate the degrees of sensor node membership to localization regions of distance-based regional map, $\mathcal{D}$, by using its membership degrees to fuzzy-ring sets. To this end, the algorithm first generates so-called *fuzzy regional map*, by combining ranks of fuzzy-rings from different fuzzy-ring sets into region area-codes. Then, the

fuzzy set of regions is derived by removing any area-code from the fuzzy regional map that does not belong to the distance-based regional map $\mathcal{D}$.

3.4.1 Fuzzy Regional Map

The fuzzy regional map is the discrete fuzzy set defined as the Cartesian product over *N* fuzzy-ring sets $\{\widetilde{RS}_k | k = 1, \dots, N\}$:

$$\widetilde{RM} = \widetilde{RS}_1 \times \widetilde{RS}_2 \times \dots \times \widetilde{RS}_N = \{(c, \mu_R(c))\}$$

Here, $c = (j_1, j_2, \dots, j_N)$ is the region area-code, such that $j_k \in \widetilde{RS}_k, k = 1, \dots, N$, and $\mu_{RM}(c)$ is the membership degree of *c* to $\widetilde{RM}$, defined as follows:

$$\mu_{RM}(c) = \prod_{k=1}^{N} \mu_{RI}^{k,j_k} \tag{4}$$

Members of $\widetilde{RM}$ are regions represented by their area-codes. The membership degree of a region to $\widetilde{RM}$ represents the certainty that the position of the sensor node falls within the area of that region. Recall that the area-code $c = (j_1, j_1, \dots, j_N)$ identifies the region in the localization space that corresponds to the overlapping area of rings whose ranks are listed in *c*. According to (4), the degree of sensor node membership to a region in $\widetilde{RM}$ is calculated by multiplying degrees of its membership to all overlapping fuzzy rings.

The size of the fuzzy regional map, i.e. the number of regions with nonzero membership degree in $\widetilde{RM}$, is equal to the product of sizes of all fuzzy-ring sets. Since each fuzzy-ring set contains at least one fuzzy ring, the number of regions in $\widetilde{RM}$ is always equal or greater than 1. In practice, the size of fuzzy regional map primarily depends on the level of fuzzification, i.e. the value of parameter *P*. An increase in the level of fuzzification will generate more fuzzy rings in fuzzy-ring sets, which will produce even more regions in $\widetilde{RM}$.

3.4.2 Fuzzy Set of Regions

It should be emphasized that not all regions in the fuzzy regional map are necessary valid, in the sense that for some of them we cannot find counterpart regions (i.e. the regions with matching area-codes) in $\mathcal{D}$. Invalid regions appear in $\widetilde{RM}$ more frequently when the radio propagation is highly irregular and/or the fuzzification is performed with a larger value of parameter *P*. On one hand, the sensor node location may be mapped into the wrong ring (or rings) due to the effect of

irregular radio propagation. On the other hand, when a higher level of fuzzification is used, the sensor node location is likely to be fuzzified into several fuzzy rings in each fuzzy-ring set. In both cases, the consequence will be an increased chance that some of resulting area-codes will include rings that do not overlap in the Euclidean domain. Since such regions do not have an adequate geometric interpretation, we filter out all of them from the fuzzy regional map, and keep for further processing only those that also belong to the distance-base regional map. Thus, the resulting fuzzy set of regions is

$$\tilde{R} = \{(c, \mu_{RM}(c)) | c \in \widetilde{RM}, c \in \mathcal{D}\}$$

In some rare cases, it may happen that the fuzzy set of valid regions, $\tilde{R}$, does not contain any area-code. This typically occurs when the fuzzification is performed with the value of parameter *P* which is not large enough to compensate for the radio propagation irregularity. Under such circumstances, there may be generated a fuzzy-ring set which only includes wrong rings which also do not overlap with any ring in some other fuzzy-ring set. In such situations, there are two options: to leave the sensor node unknown (i.e. not-localized), or to repeat the fuzzification process with a larger value of parameter *P*. In FRORF, we implement the second one.

3.5 Defuzzification

In the last step of FROFR, the fuzzy set of regions, $\tilde{R}$, is defuzzified to obtain a pair of crisp real values that represent the 2-D coordinates of estimated sensor node location. Note that two numeric attributes are associated with each area code in $\tilde{R}$: (a) the CoG of the corresponding localization region, and (b) the degree of membership in $\tilde{R}$. We use the center of gravity method to produce the final location estimation:

$$Estimated\_location = \left\{ \frac{\sum_{C \in \tilde{R}} x_{COG}(C) \cdot \mu_{RM}(C)}{\sum_{C \in \tilde{R}} \mu_{RM}(C)}, \frac{\sum_{C \in \tilde{R}} y_{COG}(C) \cdot \mu_{RM}(C)}{\sum_{C \in \tilde{R}} \mu_{RM}(C)} \right\}$$

where $x_{COG}(C)$ and $y_{COG}(C)$ are *x*- and *y*-coordinate of CoG of the region with area-code *C*.

4 SIMULATION RESULTS

We implement the FRORF localization algorithm in a custom WSN simulator build in C++, and conducted several experiments to evaluate its performance. In addition, we compare our results to the ROCRSSI algorithm. Our evaluation is based on the simulation of a benchmark set of 60

different network configurations categorized into six subsets of ten networks with the same number of anchors. We analyze network configurations with 3 to 8 anchors. All networks in one subset are created by varying positions of *N* anchors within the same basic setup of 200 sensor nodes randomly deployed in a circular area of 100 m in diameter. In our simulations, we intend to illustrate the impact of the number of anchors, the degree of radio propagation irregularity, and the level of fuzzification on the localization error. The performance of two localization methods is evaluated using the location estimation error defined as (*d*/*D*)*100%, where *d* is the Euclidian distance between the real location of a sensor node and its estimated location, and *D* is the diameter of the localization area.

4.1 Radio Propagation Model

We adopt the Degree Of Irregularity (DOI) radio propagation model introduced in [5] and subsequently extended in [19], so that it can calculate the received signal strength at any specific point within the radio range of a sender. In this model, the signal strength is defined as $C \times K(\theta)/d^2$, where C is a constant, d is the distance between the receiver and the transmitter, and $K(\theta)$ is the coefficient representing the difference in path loss in different directions. $K(\theta)$ is calculated according to (5) where $\theta \in [0, 360^0]$, *rand* is a random number uniformly distributed in the range [-1,1], $s = \lfloor\theta\rfloor$, and $s = \lceil\theta\rceil$ [19]. The parameter *DOI* is used to denote the irregularity of the radio pattern. It is defined as the maximum signal straight variation per unit degree change in the direction of radio propagation. When *DOI* value is 0, there is no variation in the signal straight which results in a perfectly circular radio model. When *DOI* > 0, large *DOI* values represent large variation of radio irregularity. Examples of two characteristic DOI values of this irregular radio pattern model are shown in Fig. 9.

$$K(\theta) = \begin{cases} 1 & \theta = 0 \\ K(\theta - 1) + rand \times DOI & \theta\ is\ positive\ integer \\ K(t) + (\theta - s) \times (K(t) - K(s)) & otherwise \end{cases} \quad (5)$$

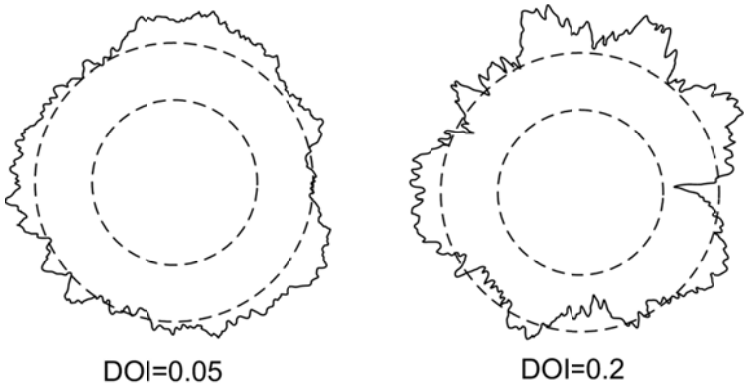

Fig. 9. Irregular radio patterns for different values of *DOI*.

4.2 Localization Error When Varying P

In order to analyze the impact of the fuzzification level, expressed by the value of parameter *P*, on the localization error we simulate FRORF algorithm under various degrees of radio propagation irregularity in a network with $N = 5$ anchors. The value of parameter *P* defines the width of the boundary region of fuzzy membership functions. When *P* value is 0, the fuzzification is practically switched-off by forcing selection of one ring per anchor, only. When *P* is greater than 0, the chance of selecting multiple rings per anchor increases. In this way, the value of *P* directly influences the size of the fuzzy set of regions. Fig. 10 shows the location error as a function of *P* for four characteristic values of *DOI*.

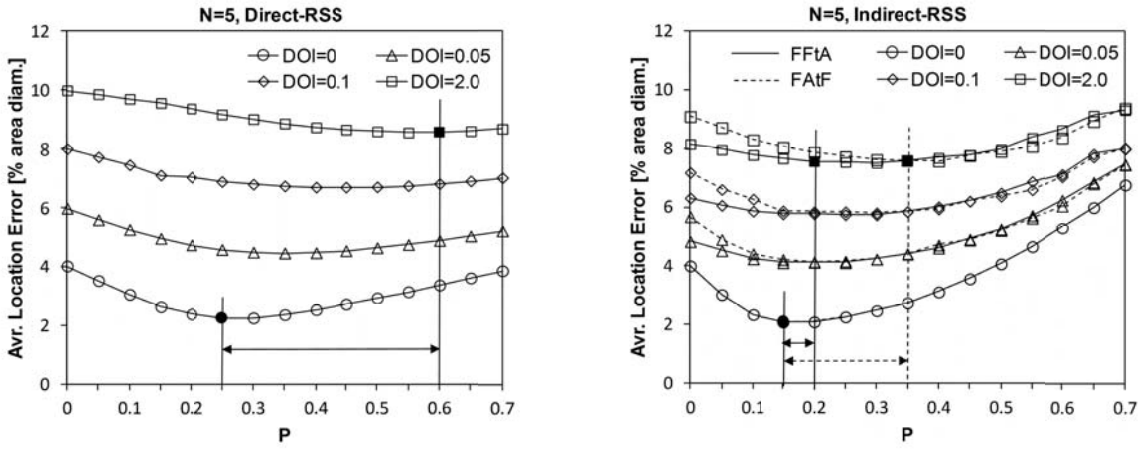

(a) (b)

Fig. 10. Localization error vs. level of fuzzification (*P*) for four different degrees of radio propagation irregularity (*DOI*): (a) FRORF, Direct-RSS fuzzification; (b) FRORF, Indirect-RSS fuzzification.

As can be seen from Fig. 10 the fuzzy approach is beneficial even in the circular radio propagation scenario (i.e. when *DOI* value is 0). The circular radio propagation pattern guaranties an ideal "1-1" matching between regions in distance-based and fuzzy regional map enabling the FRORF algorithm to always select the correct localization region, even without fuzzification (*P*=0). The only source of localization errors is due to the distance between the CoG of the selected region and the real location of the sensor node. When *P* > 0, the result of the fuzzification process is the fuzzy set of regions that includes multiple localization regions with different weights. This can move the CoG toward the real location of the sensor node. When *DOI* > 0, the irregular radio propagation creates rings with non-circular borders causing a non-ideal mapping between distance-base and fuzzy localization regions. Without the fuzzification (*P*=0), the localization error is influenced not only by the inter-region errors but also by the wrong ring selection. On the other hand, with the fuzzification switched-on (*P*>0), the fuzzy set of regions will likely include the correct region along with several nearby regions, which will partially compensate the inaccuracy of RSS measurements.

As can also be seen from Fig. 10, for every value of DOI and every FRORF variant, there is an optimal value of the parameter *P*, P_{opt}, for which the best performance is achieved. The P_{opt} increases with the increase of DOI value because the membership functions with wider fuzzy regions are needed to compensate for increased uncertainty in ring/region selections. When the direct-RSS fuzzification is employed, and DOI varies from 0 to 0.2, the range of optimality for *P* is from 0.25 to 0.6 (Fig. 10(a)). This range is narrower when the indirect-RSS fuzzification is used (Fig. 10(b)), i.e. $P_{opt} \in [1.5, 2.0]$, for FFtA, and $P_{opt} \in [1.5, 3.5]$, for FAtF. The narrow optimality range for *P* is an advantage of indirect- over direct-RSS fuzzification method, which is reflected in the extent to which the localization performance of the algorithm is resilient to variations in the degree of the radio propagation irregularity. For example, when the FFtA is configured with *P* = 0.2, the additional localization error due to non-optimal selection of *P* value is less than 0.1% of area diameter over the analyzed range of DOI. This additional error for FAtF is up to 0.2% when *P* value is 0.25, and up to 0.3% for direct-RSS fuzzification when *P* value is 0.35.

4.3 Localization Error When Varying Number of Anchors

In this simulation setting, we study the influence of the number of anchors, *N*, on the localization error. We apply both ROCRSSI and FRORF algorithms to all network configurations in the benchmark set with $DOI \in \{0, 0.05, 0.1, 0.2\}$. Fig. 11 shows the location errors as a function of the number of anchors deployed. Each data point in these graphs represents the average value of

20.000 localization trials. First, for every *N* we simulate 10 different anchor configurations within the network of 200 sensor nodes. Second, for each anchor configuration, 10 runs with different random seeds for DOI were executed.

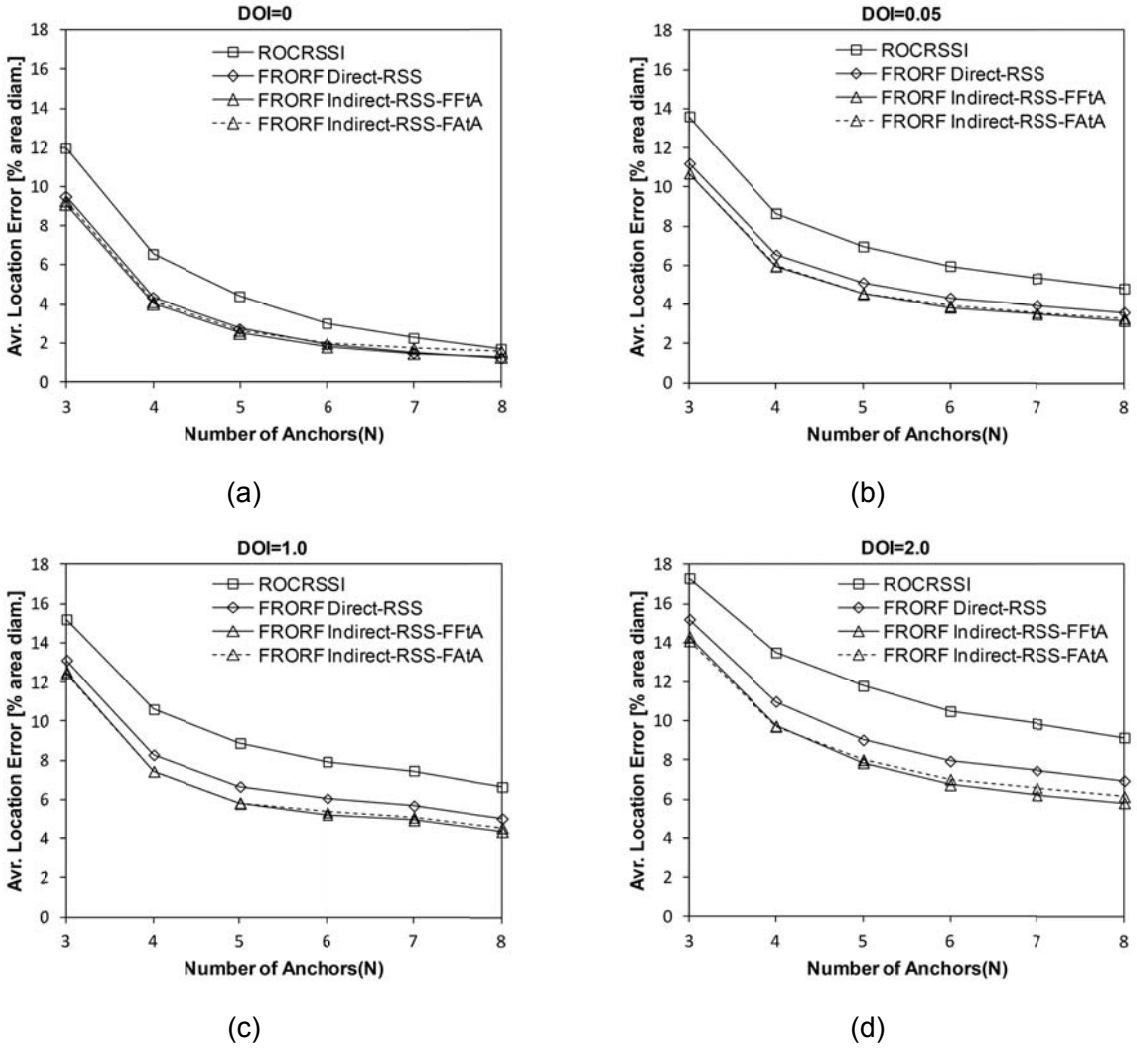

Fig. 11. Localization error vs. number of anchors for: (a) *DOI* = 0; (b) *DOI* = 0.05; (c) *DOI* = 0.1; (d) *DOI* = 0.2.

From Fig. 11, we see that our proposed localization method presents a clear performance advantage over the ROCRSSI, no matter whether the radio propagation is regular (DOI=0) or irregular (DOI=0.2). For example, when we set the number of anchors to 5, the relative performance improvement of the FRORF algorithm with direct-RSS fuzzification over ROCRSSI ranges from 23% (for DOI=0.2) up to 37% (for DOI=0). Therefore, FRORF algorithm enables us to deploy a smaller number of anchors to obtain the same level of performances as with ROCRSSI. For example, the direct-RSS FRORF only needs 5 anchors to achieve the same

localization error as ROCRSSI with 8 anchors. From Fig. 11, we can also see that the indirect-RSS fuzzification is able to provide even better performance than direct-RSS, especially in the presence of highly irregular radio pattern. The relative performance improvement of FFtA over ROCRSSI ranges from 33% (for DOI=0.2) up to 43% (for DOI=0). On the other hand, the performance difference between two indirect-RSS variants, FFtA and FAtF, is rather insignificant, except for a larger DOI and a larger number of anchors when FFtA outperforms FAtF for at most 5%.

4.4 The Influence of DOI

In this experiment, the results of which are shown in Fig. 12, we quantify the degree of localization performance degradation in the presence of radio irregularity. We conduct the analysis on the network configuration with *N*=5 anchors under various degrees of radio propagation irregularity.

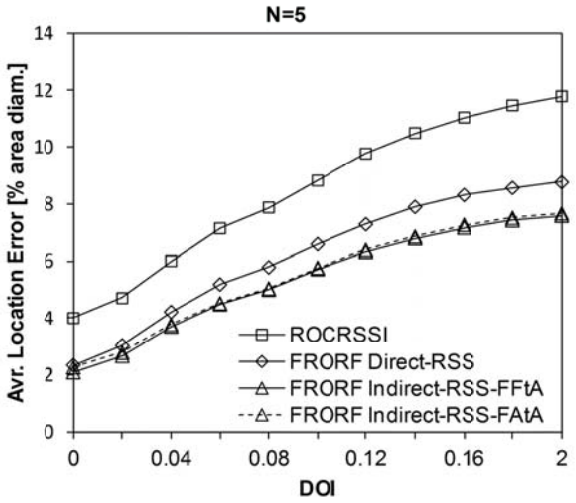

Fig. 12. Localization error vs. degree of radio propagation irregularity for ROCRSSI and FRORF algorithms.

From Fig. 12, we observe that the location error of both ROCRSSI and FRORF increases rapidly when DOI value increases and FRORF performs much better then ROCRSSI particularly in the presence of highly irregular radio propagation. When DOI value is 0, the radio propagation patter is circular and localization performances of all three analyzed FRORF fuzzification methods are practically the same, reducing the average location error by 1.8% of the area diameter with respect to ROCRSSI. As DOI increases, the performance differences among analyzed localization schemes become larger. So, when DOI=0.2, the direct-RSS FRORF estimates the sensor node location with the average error of 8.7% of area diameter, which is an improvement

of 3% of area diameter with respect to ROCRSSI. Note that indirect-RSS fuzzification approach outperforms direct-RSS approach in the whole range of analyzed DOI values, reducing the location error for additional 1.2% of area diameter, when DOI is 0.2.

5 CONCLUSION

Many applications of wireless sensor networks depend on accurate determination of the positions of all network nodes. In this paper, we describe and investigate a new RSS-based range-free localization method, called Fuzzy Ring Overlapping Range Free (FROFR) localization. The novelty of our scheme is to combine ROCRSSI, a ring-overlapping approach originally proposed in [19], and the fuzzy set theory for performing sensor localization. Fuzzy set theoretical approach helps to manage uncertainty associated with RSS measurement more efficiently with fewer anchors. Simulation results show that FRORF performs better than ROCRSSI in terms of localization accuracy by about 15-30% under different number of anchors and degrees of radio propagation irregularity. We also show that FRORF improves range-free localization under ideal radio propagation model. However, due to the implemented fuzzy logic approach, it is important to notice that FRORF has increased computational cost comparing to ROCRSSI method. With little overhead, FRORF can be conveniently embedded in different area-based localization algorithms to improve accuracy.

This paper does not consider the way to adapt the level of fuzzification to the varying degree of radio propagation irregularity. This remains for a future work. We want to implement also self-calibration scheme in order to improve performance of the FROFR. In our future work, we would also like to test the proposed scheme under more network scenarios such as limited radio range of anchors, and to study the effect of topology of anchor nodes on localization error. It is planned to implement FRORF method on the WSN platform and provide field test results.

Acknowledgements

This research was sponsored in part by the Serbian Ministry of Science and Technological Development, project no. TR-32009 - "Low-Power Reconfigurable Fault-Tolerant Platforms".

6 REFERENCES

[1] F. Akyildiz, W. Su, Y. Sankarasubramaniam, and E. Cayirci, Wireless sensor networks: A survey, *Computer Networks* **38** (3) (2002), pp. 393–422.

[2] H. Karl and A. Willing, Protocols and Architectures for Wireless Sensor Networks, John Wiley & Sons, 2005.

[3] B. H. Wellenhoff, H. Lichtenegger and J. Collins, Global Positions System: Theory and Practice, *fourth ed.*, Springer Verlag, 1997.

[4] D. Nicolescu and B. Nath, DV based positioning in ad hoc networks, *Journal of Telecommunication Systems* **22** (1) (2003), pp. 267–280.

[5] T. He, C. Huang, B.M. Blum, J. A. Stankovic and T. Abdelzaher, Range-Free Localization Schemes for Large Scale Sensor Networks, in: Proceedings of the 9th annual international conference on Mobile computing and networking (MobiCom 2003), San Diego, California, 2003, pp. 81-95.

[6] G. Mao, B. Fidan and B. Anderson, Wireless Sensor Networks Localization Techniques, *Computer Networks* **51** (10) (2007), pp. 2529-2553.

[7] R. Peng and M. L. Sichitiu, Angle of arrival localization for wireless sensor networks, in: Proceedings of the 3th annual IEEE Communications Society conference on Sensor and Ad Hoc Communications and Networks, Reston, VA, 2006, vol. 1, pp. 374-382.

[8] Y. Kwon, K. Mechitov, S. Sundresh, W. Kim, and G. Agha, Resilient Localization for Sensor Networks in Outdoor Environments, in: Proceedings of the 25th IEEE International Conference on Distributed Computing Systems (ICDCS), 2005, pp. 643-652.

[9] Y.-T. Chan, W.-Y. Tsui, H.-C. So, and P. Ching. Time of arrival based localization under NLOS conditions. *IEEE Transactions on Vehicular Technology,* **55** (1) (2006), pp. 17-24.

[10] G. Zhou, T. He, S. Krishnamurthy and J.A. Stankovic, Impact of radio irregularity on wireless sensor networks, in: Proceedings of 2nd international conference on Mobile Systems, Applications, and Services, 2004.

[11] T. Pavani, G. Costa, M. Mazzotti, D. Dardari and A. Conti, B, Experimental results on indoor localization techniques through wireless sensors network, in: Proceedings of the IEEE 63rd Vehicular Technology Conference (VTC 2006-Spring), 2006, vol. 2, pp. 663–667.

[12] K. Whitehouse, C. Karlof, and D. Culler. A Practical Evaluation of Radio Signal Strength for Ranging-based Localization. *ACM SIGMOBILE Mobile Computing and Communications Review* **11** (1) (2007), pp. 41-52.

[13] R. Stoleru, T. He, and J. A. Stankovic, Range-free Localization, in: R. Poovendran, C. Wang, and S. Roy (Eds.), Secure Localization and Time Synchronization for Wireless Sensor and Ad Hoc Networks, Advances in Information Security series, vol. 30, Springer-Verlag New York, Inc., 2007. Part I, pp. 3-31.

[14] N. Bulusu, J. Heidemann, and D. Estrin, GPS-less low-cost outdoor localization for very small devices, *IEEE Personal Communications,* **7** (5) (2000), pp. 28 -34.

[15] V. Vivekanandan and V. W. S. Wong, Concentric Anchor Beacon Localization Algorithm for Wireless Sensor Networks, *IEEE Transactions on Vehicular Technology*, **56** (5) (2007), pp. 2733-2744.

[16] H.Chen, Q. Shi, R. Tan, H. V. Poor, and K. Sezaki, Mobile Element Assisted Cooperative Localization for Wireless Sensor Networks with obstacles, *IEEE Transactions on Wireless Communications*, **9** (3) (2010), pp. 956-963.

[17] R. Nagpal, H. Shrobe, and J. Bachrach, Organizing a global coordinate system from local information on an ad hoc sensor network, *2nd International Workshop on Information Processing in Sensor Networks (IPSN '03)*, Palo Alto, pp. 333-348, Apr. 2003.

[18] Z. Zhong and T. He, “RSD: A Metric for Achieving Range-Free Localization beyond Connectivity,” IEEE Transactions on Parallel and Distributed Systems, **22**, (11) (2011), pp. 1943-1951.

[19] C. Liu, T. Scott, K. Wu and D. Hoffman, Range-free sensor localization with ring overlapping based on comparison of received signal strength indicator, *International Journal of Sensor Networks (IJSNet)*, **2** (5) (2007), pp. 399-413.

[20] Hyo-Sung Ahn; Wonpil Yu, Environmental-Adaptive RSSI-Based Indoor Localization, *IEEE Transactions on Automation Science and Engineering,* **6** (9) (2009), pp 626 – 633.

[21] S. Yun, J. Lee, W. Chung, E. Kim, Centroid localization method in wireless sensor networks using TSK fuzzy modeling, in: Proceedings of International symposium on Advanced Intelligent Systems, Sokcho, Korea, 2008, pp. 971–974.

[22] S. Yun, J. Lee, W. Chung, E. Kim and S. Kim, A soft computing approach to localization in wireless sensor networks, *Expert Systems with Applications Journal* **36** (2009), pp. 7752-7561.

[23] F. Sivrikaya and B. Yener, Time synchronization in sensor networks: a survey, *IEEE Network*, **18** (4) (2004), pp. 45-50.

[24] D. J. Dubois and H. Prade, *Fuzzy Sets and Systems: Theory and Applications*, Academic Press, New York, 1980.